

Electrical stimulation at the dorsal root ganglion preserves trabecular bone mass and microarchitecture of the tibia in hindlimb-unloaded rats

Y.-C. Lau · X. Qian · K.-T. Po · L.-M. Li · X. Guo

Received: 15 April 2014 / Accepted: 19 August 2014 / Published online: 12 September 2014
© International Osteoporosis Foundation and National Osteoporosis Foundation 2014

Abstract

Summary This study seeks to investigate the effect of electrical stimulation (ES) at dorsal root ganglion (DRG) on disuse bone loss in a rat model. Hindlimb unloading for 14 days resulted in significant bone loss in rat tibia while rats with ES at DRG showed a significant reduced bone loss

Introduction Mechanical unloading induces osteoporosis in both human and animals. Previous studies demonstrated that electrical stimulation (ES) to dorsal root ganglion (DRG) could trigger secretion of calcitonin gene-related peptide (CGRP) which plays an important role in bone modeling and remodeling. This study seeks to investigate the effect of ES to DRG on disuse bone loss in a rat model.

Methods Twenty-four rats were randomly assigned in three experimental groups: cage control (CC), hindlimb unloading (HU), and hindlimb unloading with ES (HUES). ES was applied via implantable micro-electrical stimulators (IMES) to right DRGs at vertebral levels L4–L6 in HUES group.

Results Hindlimb unloading for 14 days resulted in 25.9 % decrease in total bone mineral content (BMC), 29.2 % decrease in trabecular BMD and trabecular microarchitecture and connectivity were significantly deteriorated in the proximal tibia metaphysis in HU group, while rats with ES at DRG showed significant reduced bone loss that there was 3.8 % increase in total BMC, 2.3 % decrease in trabecular BMD, and significant improvement in trabecular microarchitecture. There was a concurrent enhancement of expression of CGRP in stimulated DRGs.

Conclusions The results confirm the effect of ES at DRG on enhancing CGRP expression and suggest potential applications of IMES for the prevention and treatment of disuse bone loss.

Keywords Bone mineral density · CGRP · Disuse osteoporosis · Dorsal root ganglion · Electrical stimulation

Introduction

Bone is a metabolically active tissue that adapts its structure and mass in response to mechanical stimuli. Disuse or reduction in mechanical loading causes an imbalance in bone turnover, with bone resorption favored over bone formation, and thus a rapid loss of bone mass, which results in disuse osteoporosis. It has been well documented in both humans and animal models that bone loss following unloading of the weight-bearing bones [1–3], for instance, decrease in trabecular bone mass in the tibia in astronauts following 4 weeks to several months spaceflight [4], bone loss in rats subjected to hindlimb unloading for 2 weeks [5]. Lecoq et al. [6] compared the bone loss in female rats induced by hindlimb unloading, ovariectomy, and the combined effect of both treatments. Their results showed that hindlimb unloading induced a greater degree of bone loss than estrogen deprivation.

While it has been long appreciated that mechanical force is one of the crucial regulators of bone remodeling and repair, the actual mechanism by which physical force is converted into intracellular biological signal(s) remains largely unexplained. Calcitonin-gene-related peptide (CGRP) is a sensory neuropeptide that shares the same encoding gene complex as calcitonin. Calcitonin is produced when the gene is expressed in C cells in the thyroid, while CGRP is produced when the same gene is expressed in sensory neurons located in the dorsal root ganglion (DRG). CGRP is then transported

Y.-C. Lau · K.-T. Po · X. Guo (✉)
Department of Rehabilitation Sciences, The Hong Kong Polytechnic University, Hung Hom, Hong Kong, China
e-mail: xia.guo@polyu.edu.hk

X. Qian · L.-M. Li
School of Aerospace, Tsinghua University, Beijing, China

peripherally and co-stored in large electron-dense storage vesicles, the accumulation of which constitutes varicose enlargements of the sensory axon [7]. Numerous *in vitro* studies have suggested that CGRP modulates the activities of bone cells [8–10], including both osteoblasts and osteoclasts. CGRP causes a 30 to 500-fold increase in osteoblastic cyclic adenosine monophosphate (cAMP) by interacting with osteoblast specific CGRP receptors, thus stimulating osteogenesis [8]. CGRP also acts directly on osteoclasts to inhibit bone resorption [9]. These *in vitro* bone metabolism-associated properties of CGRP, together with morphologic evidence of CGRP-containing fibers in bone, suggest the modulatory roles of osseous CGRP-containing fibers and their specific function. The modulatory effect of CGRP-containing fibers on bone metabolism has been studied by Zaidi et al. [7], who reported that high doses of CGRP significantly inhibited bone resorption in rats. Moreover, another study demonstrated that transgenic mice with osteoblasts expressing CGRP had higher trabecular bone density and bone volume than those in transgenic negative controls [9].

Brooks et al. [11] showed that CGRP secretion could be triggered by electrical stimulation (ES) at dorsal root. CGRP plays important role in bone formation and remodeling. However, it is unclear whether ES at the DRG-induced increases in CGRP secretion can prevent disuse bone loss.

We hypothesized that ES at the DRG triggers increased CGRP secretion by DRG neurons, reducing disuse bone loss. Therefore, the primary objective of this study was to determine the effect of ES at the DRG on CGRP expression and tibiae bone quantity in hindlimb-unloaded rats. The outcome of this study will provide the scientific foundation for ES to sensory nerves to prevent disuse osteoporosis.

Methods

Animals

Twenty-four Sprague Dawley rats (3 months old; weight, 420–450 g) were randomly assigned into three groups ($n=8$ per group): the cage control (CC), hindlimb unloaded (HU), and hindlimb unloaded with ES to the DRG groups (ES). All animals were housed individually in metal cages and were provided with unlimited access to food and water. The environment was maintained with a 12 h day–night cycle at 24 °C. The protocol of animal care and experiment was approved by the Animal Ethics Committee of The Hong Kong Polytechnic University. Electrical stimulation to the DRG of ES rats was generated by a set of implantable micro-electrical stimulators (IMES) implanted in the spinal region. The duration of experiments was 2 weeks. After the treatment period, animals were euthanized by CO₂ inhalation. The spinal cord at vertebral levels L4 to L6 with bilateral DRGs and right tibiae were

harvested and fixed in 4 % paraformaldehyde for 48 h, and then stored in 70 % ethanol until further use.

Hindlimb unloading protocol

The tail of a rat was suspended using a tail harness that raised its hindlimbs and kept it in a head-down position (Fig. 1a). The animals were free to move with their forelimbs. The angle formed between the body of the rat and the floor of the cage was 30°, preventing the animals from contacting the ground and bearing weight on their hindlimbs and providing normal weight bearing on the forelimbs, unloaded the lumbar vertebrae but not the cervical vertebrae [12, 13].

Implantation of IMES and stimulation protocol

ES was generated by an IMES developed by the Department of Aeronautics & Astronautics Engineering, Tsinghua University, China [14, 15]. An IMES unit consists of a body containing the circuit board and a button-type battery, three electrodes, and wires connecting the body and the electrodes (Fig. 1b). The dimensions of the body are 25 mm×20 mm×8 mm, and the weight is 5.86 g. In order to resist corrosion of electrical components in the physiological environment, the body is coated with poly-para-xylylene (parlylene C) and silicone rubber. The body is connected to three coaxial electrodes. The outer layer of each electrode is a stainless steel

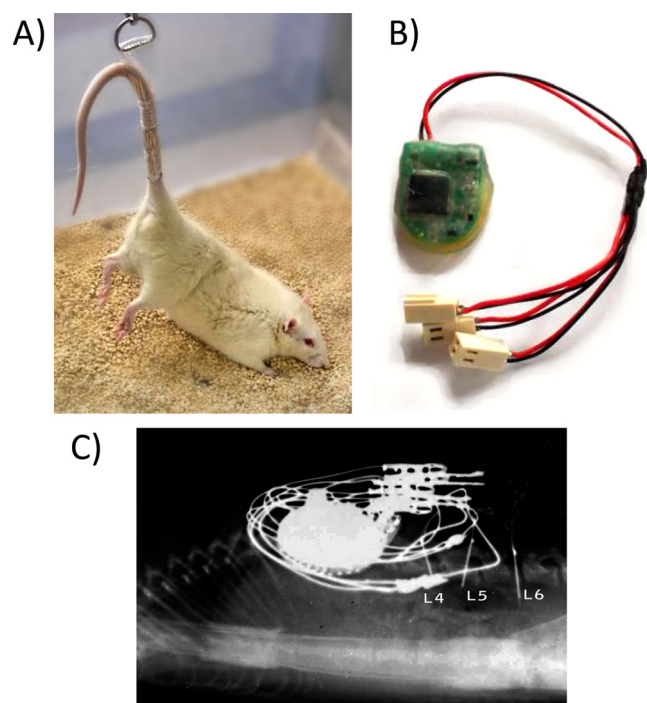


Fig. 1 **a** Hindlimb-unloaded model. **b** Implantable micro-electrical stimulator. **c** X-ray showing position of the IMES and electrodes implanted at right DRGs at the level L4–L6

tube that serves as a reference pole, while the electrode core is fitted with a stainless steel wire coated with a layer of parylene. The uncoated tip of the core serves as the negative polarity stimulating pole. The implanted stimulator unit is externally controlled with a remote control unit. Treatment parameters, including stimulation frequency, pulse duration, stimulation voltage, and on- and off-times, can be adjusted with the remote control unit.

ES was applied to the right DRGs at vertebral levels L4 to L6, including sensory neurons that innervate the tibial and common peroneal regions of the right hindlimbs in rats [16]. Implantation of the IMES was carried out under general anesthesia with an intraperitoneal injection of ketamine (10 %) and xylazine (2 %; volume ratio, 2:1; dosage, 0.1 ml per 100 g body mass). The right transverse processes of L4 to L6 were exposed through a dorsal incision, and 1 mm diameter holes were drilled at the DRG on the right transverse processes (Fig. 2). After the electrodes were inserted into the holes, they were sutured to the muscle, fixing their positions. The body of the stimulator was implanted subcutaneously in the lower back area in such a way as to create the least motion restriction for the animal. The electrodes were then connected to the body. The positions of the electrodes and body were monitored by X-ray imaging during the treatment period (Fig. 1c).

The ES signal was a rectangular pulse waveform at constant amplitude [15]. The pulse width, frequency, current, and voltage of the electrical stimulation applied were 90 μ s, 150 Hz, 61.3 μ A, and 0.25 V. The stimulation voltage used in this study was defined as the maximum stimulation voltage applied without triggering visible muscular contraction in the innervated muscles since electrically induced muscle contractions were expected to reduce bone density decline [17]. The stimulation signals were verified by an *in vivo* validation procedure that the stimulation signals were detected by a recording electrode implanted at the transverse process

2 mm anterior to the site of stimulation. The recording electrode was connected to an oscilloscope (Tektronix MSO 4104, Tektronix Inc.), which measured and recorded the electrical stimuli detected. Based on our observations, no muscle contraction was induced when a stimulation voltage of 0.25 V was applied, but *in vivo* electrical signals were still detectable. In the ES group, each animal was stimulated 20 min per day for 14 days.

Immunohistochemistry

Harvested specimens of spinal cord and DRG were rehydrated in 0.01 M phosphate-buffered saline (PBS) containing 20 % sucrose for 5 h at room temperature. Then, the DRG samples were sectioned at a thickness of 7 μ m on a cryostat. The immunohistochemical staining was performed following an established protocol [18]. Briefly, the DRG sections were treated in 0.5 % horse serum (Life Technologies, Carlsbad, CA, USA) for 30 min at room temperature. The sections were then incubated with rabbit antibody to CGRP (1:50, Abcam, Cambridge, MA, USA) for 24 h at 4 °C, followed by incubation with goat anti-rabbit Alexa Fluor 555 fluorescent antibody conjugate for visualization (1:1,000; Life Technologies, Carlsbad, CA, USA). Finally, the sections were mounted with aqueous-based mounting agent with 4', 6-diamidino-2-phenylindole (DAPI, Vector Laboratories Inc., Burlingame, CA, USA). The sections were examined using a fluorescence microscope (Nikon eclipse 80i; Nikon, Tokyo, Japan) immediately after immunostaining. The fluorescence microscope was equipped with a mercury lamp and appropriate excitation filters for the red fluorescent signal of CGRP (excitation range, 550 to 590 nm) [19] and for the blue DAPI signal (excitation ~360 nm) [20].

The captured images of labeled DRG sections were further analyzed using ImageJ version 1.46r (National Institutes of Health, Bethesda, MD, USA). To calculate the number of CGRP+neurons, 100 fluorescent images of the right side DRGs were selected per animal at random, and the number of CGRP+neurons was counted. Only CGRP+neurons with visible nuclei were included in the count. The total area of CGRP fibers was quantitatively evaluated. The intensity of the CGRP-signal and the number of pixels within a region of interest (ROI) were generated using the built-in histogram function of the ImageJ software. The area of the ROI was estimated as the proportion between the number of pixels within the ROI and the total number of pixels captured. Significantly enhanced signals (CGRP++) were further defined as signals with intensities more than 2 standard deviations higher than the mean ROI intensity. The proportion of CGRP++ neurons was then estimated.

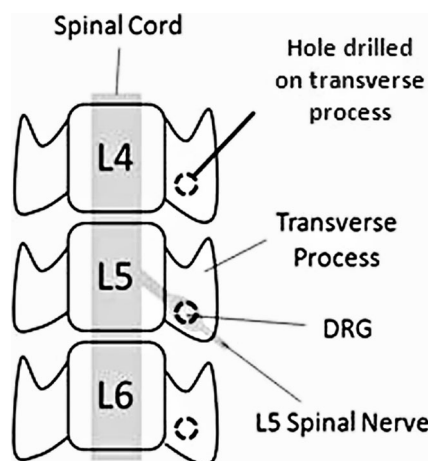


Fig. 2 Locations of holes drilled on transverse processes for insertion of electrodes

Peripheral quantitative computed tomography (pQCT)

Tomographic scans of tibiae were performed *in vivo* before treatment and *ex vivo* after harvesting the bone samples using a peripheral quantitative computed tomography (pQCT) scanner with software version 5.2 (Stratec XCT2000, Norland, USA). Each tibia was cross-sectionally scanned at 2, 3, and 4 mm from the proximal end of the bone, regions rich in cancellous bone. Another three slices were scanned at the midpoint of the total length of the tibia. Standardized analyses for either the metaphyseal region (contour mode 3, peel mode 2; outer attenuation threshold, 0.214 g/cm³; inner attenuation threshold, 0.605 g/cm³) or diaphyseal region (separation 1; attenuation threshold, 0.605 g/cm³) were applied to each slice obtained [21]. The total bone mineral content (BMC) and total, cortical, and cancellous bone mineral densities (BMD) were measured in the metaphyseal region, and cortical BMC and BMD were measured in the diaphyseal region. The parameters in the slice with the highest total BMD values at each site were used for further analyses.

Micro-computed tomography (μ CT)

The harvested tibiae were scanned with a high resolution μ CT (μ CT-40, SCANCO Medical AG, Bassersdorf, Switzerland).

The basic parameters were set as following: voltage 70 kV, current 114 μ A, and integration time 170 ms. The proximal metaphysis of the tibiae was scanned at a resolution with an isotropic voxel size of 19 and 38 μ m, respectively. In order to suppress the noise in the results, all images were evaluated with a constrained 3D Gaussian filter (filter width, $\sigma=1.2$; filter support, $S=2$). The volume of interest (VOI) at proximal metaphysis was defined as the 200 μ m region beginning at 100 μ m below the growth plate. The threshold value for proximal metaphysis was 250 mg/cm³. All scans were reconstructed with the same parameters for different portions. The quantitative analysis of trabecular bone microarchitecture included the following indices at the proximal metaphysis: bone volume fraction (BV/TV), connectivity density (Conn.D), structural model index (SMI), trabecular number (Tb.N), thickness (Tb.Th), and separation (Tb.Sp).

Statistical analysis

Statistical analysis was performed using SPSS ver.20 (IBM, Armonk, NY, USA). The results are presented as mean \pm standard deviation. Percentage changes in bone quality parameters between pre- and post-treatment measurements in each group were calculated using Eq. 1:

$$\text{Change in bone quality parameter (\%)} = 100\% \times \frac{\text{bone quality parameter at day 14} - \text{bone quality parameter at day 0}}{\text{bone quality parameter at day 0}} \quad (1)$$

To determine whether stimulation to the DRG had an effect on bone mass and structure, intergroup differences in BMC and BMD changes measured in the right tibiae and structural parameters were evaluated using one-way ANOVA with LSD post-hoc tests. Statistical significance was accepted as $p < 0.05$.

Results

pQCT

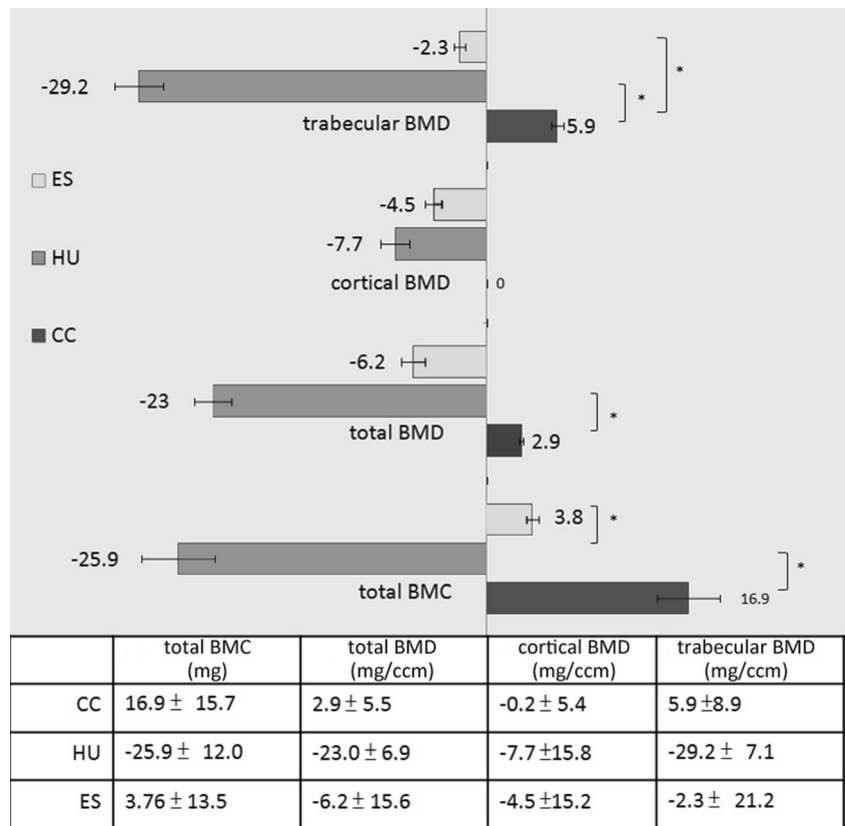
The total BMC in the proximal right tibia increased in the CC and ES groups, while it decreased in the HU group. Comparing the percentage change in parameters measured from the right tibiae among the three groups, significant bone loss in terms of reduced total BMC, as well as total and trabecular BMD, was observed in the proximal tibiae in the HU group compared with the CC ($p < 0.05$) and ES groups ($p < 0.05$), while there was no significant difference

in these measurement between CC and ES groups ($p > 0.05$). There was no significant difference in cortical BMD and BMC of diaphysis among the three groups ($p > 0.05$; Fig. 3).

microCT

Upon 2 weeks of hindlimb unloading, it is shown by one-way ANOVA and post-hoc LSD tests, significantly reduced BV/TV ($p=0.038$), Conn.D ($p=0.008$), Tb.N ($p=0.034$), and increased Tb.Sp ($p=0.044$) in the HU group compared to the CC group. In addition, larger SMI ($p=0.011$) was estimated in the HU group indicating increased rod-like structure of trabeculae upon unloading (Table 1). In the ES group, reduced deterioration of micro-architecture at the trabecular compartment of proximal tibial metaphysis was observed. Although significantly lower Conn.D ($p=0.032$) and larger SMI ($p=0.044$) were found in the ES group compared to the CC group, no significant difference in other micro-structural parameters existed between the ES and CC groups (Table 1).

Fig. 3 Percentage change in bone mass measurements of right tibiae. *CC* cage control, *HU* hindlimb unloaded, *ES* hind limb unloaded with electrical stimulation at DRG. * $p < 0.05$



Immunohistochemistry

At day 14 of experiment, CGRP+neurons in the DRG were visualized by immunohistochemistry. On the right side, according to the results of one-way ANOVA and post-hoc LSD test on the proportion of CGRP+neuron in DRG, HU group was significantly lower than both CC (Fig. 4a–c; $p < 0.05$) and ES group (Fig. 4g–i; $p < 0.05$), while there was no significant difference between the ES and CC groups ($p > 0.05$) (Table 2). However, the proportion of CGRP+neuron in left DRG of CC was significantly higher than that of both HU and ES (one-way ANOVA with post-hoc LSD test, $p < 0.05$; Table 2), whereas no difference in proportion of CGRP+neuron existed

between left DRG of HU and ES (Fig. 5). Evaluation of the intensity of CGRP signals showed that CGRP++ neurons (Fig. 4h) presented only in right DRGs of ES group but not in CC and HU groups nor left DRGs of ES group. The proportion of CGRP++ neurons in ES group was $15.5 \pm 5.6\%$, accounted for 91.2 % of CGRP+neurons. The enhanced CGRP signal complied with the occurrence of DAPI signals (Figs. 4g–i and 5g–i), where DAPI bound DNA and produced fluorescent signals upon excitation.

Table 1 Micro-architectural parameters of proximal metaphysis of right tibia

	CC	HU	ES
BV/TV (%)	20.51±4.46	11.74±6.53 ^a	13.46±4.03
Conn.D (#/mm ³)	81.84±20.38	33.21±25.38 ^a	45.71±12.67 ^a
SMI(#)	2.17±0.20	2.70±0.32 ^a	2.56±0.15 ^a
Tb.N (#/mm)	3.80±0.83	2.80±0.94 ^a	3.07±0.66
Tb.Th (µm)	0.078±0.002	0.072±0.007	0.073±0.006
Tb.Sp (µm)	0.26±0.067	0.38±0.130 ^a	0.33±0.091

Values were means±SD

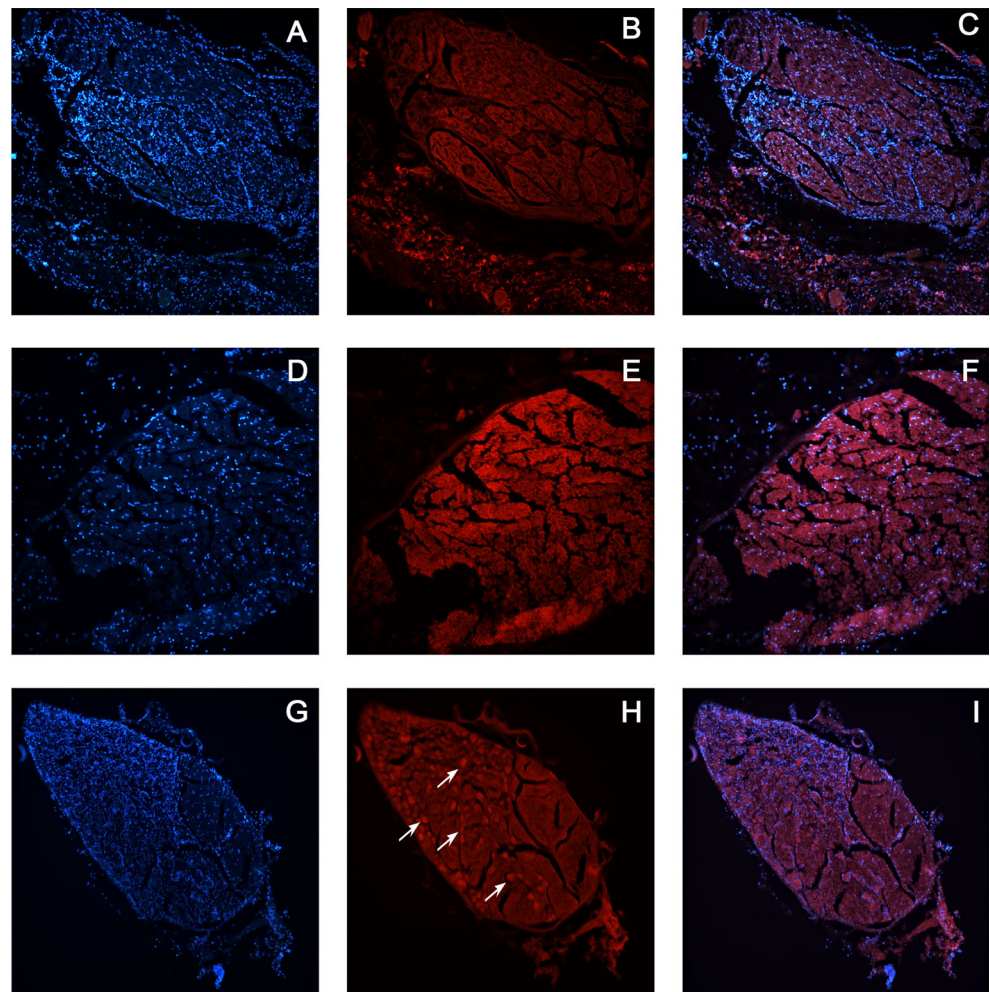
^a Significant difference ($p < 0.05$) against cage control

Discussion

The neuroplasticity of CGRP expressing neurons in the DRG

The results of this study demonstrate the expression of CGRP in the L4–L6 DRGs reduced when there is absence of mechanical loading to the hind limbs, and can be enhanced by electrical stimulation at DRG. This finding suggests the neuroplasticity and electro-excitability of CGRP expressing sensory neurons. In a study by Brooks et al. [11], electrical stimulation was applied on rat spinal cord slices *in vitro*. Using stimulation parameters of 20 V, 0.5 ms, and 10 Hz, they were able to reliably evoke release of CGRP-like immunoreactivity. Their parameters differed from those adopted in the present study (0.25 V, 90 µs, 150 Hz, and 61.3 µA) suggesting that

Fig. 4 Immunofluorescent images of right DRG ($\times 200$). **a, b,** and **c** show fluorescent signals in control (CC) DRG, whereas **d, e,** and **f** show signals in DRG of hindlimb-unloaded (HU) group. **g, h,** and **i** show fluorescent signals in electrical stimulated (ES) DRG. DAPI-labeled nuclei signals (**a, d,** and **g**). CGRP-immunoreactive signals (**b, e,** and **h**). Combined images of DAPI and CGRP signals (**c, f,** and **i**). Arrows indicate CGRP++ signals



excitation of CGRP+neurons can be achieved using a wide range of stimulation parameters. To our knowledge, this is the first report using IMES to provide electrical stimulation to the DRG for preventing bone loss. Noninvasive electrical stimulation has poor spatial resolution [22]. By comparing the occurrence of enhanced CGRP signals, the enhancement of CGRP expression was localized only in the stimulated DRG, not in non-stimulated DRG. These results suggest that IMES can achieve *precise* electrical neurostimulation. *Precise* neurostimulation has applications for both the basic understanding of neural functions and in the clinic as a diagnostic or

therapy. In addition, comparing the CGRP expression between right (Fig. 4) and left DRGs (Fig. 5), enhanced CGRP signal could not be observed in the left DRG in the absence of electrical stimulation. This suggested further that the effects on CGRP expression were localized only to region affected by stimulation.

The effect of imes on disuse bone loss

Bone loss in bones of lower limbs following unloading is well documented. It was demonstrated that the impact of short period unloading and electrical stimulation at the DRG on the bone mass and microarchitecture in rats. After 14 days of hindlimb unloading, dramatic declines in total BMC and trabecular BMD occurred in the proximal tibia metaphysis. These results agreed with the findings reported in previous studies [6, 21] that a fast decrease in BMD of cancellous bone occurs following hindlimb unloading. The bone loss in trabecular bone at the microarchitectural level was illustrated by a significant decrease in BV/TV, Conn.N, and Tb.N, and increase in Tb.Sp and SMI. The most significant change was

Table 2 Average proportion of CGRP+neuron in DRG

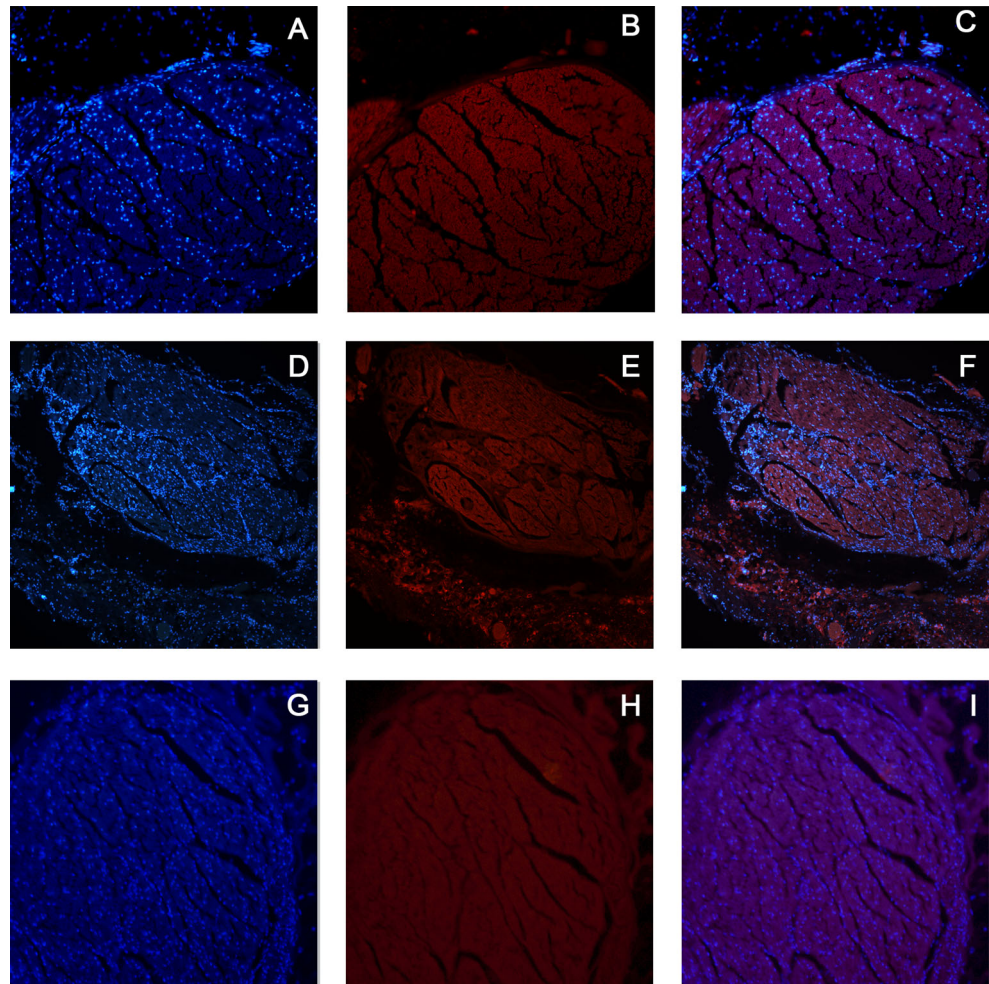
	CC	HU	ES
CGRP+neuron in right DRG [%]	17.8±1.2	14.8±0.6 ^a	18.8±1.7 ^b
CGRP+neuron in left DRG [%]	18.0±0.03	14.7±0.01 ^a	14.5±0.02 ^a

Values were means±SD

^a Significant difference ($p < 0.05$) against cage control

^b Significant difference ($p < 0.05$) against hindlimb unloaded

Fig. 5 Immunofluorescent images of left DRG ($\times 200$). **a, b,** and **c** show fluorescent signals in control (CC) DRG whereas **d, e,** and **f** show signals in DRG of hindlimb-unloaded (HU) group. **g, h,** and **i** show fluorescent signals in electrical stimulated (ES) DRG. DAPI-labeled nuclei signals (**a, d,** and **g**). CGRP-immunoreactive signals (**b, e,** and **h**). Combined images of DAPI and CGRP signals (**c, f,** and **i**). Absence of CGRP⁺⁺ signals in ES group (**g, h,** and **i**)



the 59.6 % decrease in Conn.N which is one of the most important characteristics in explaining variance in trabecular strength. In evaluating the effects of electrical stimulation at the DRG on the bone loss, the decreases in trabecular BMC and BMD in the ES group were significantly less than those in the HU group. Microstructural parameters including BV/TV, Tb.N, and Tb.Sp were significantly improved. Conn.N decreased 44.1% in ES group, less than the 59.6 % decrease in HU group, but there was no significant difference. The overall outcome suggests that electrical stimulation to the DRG can effectively prevent deterioration of bone quality caused by unloading. There is association between enhancement of CGRP expression in the DRG and improvements in the bone quality in the ipsilateral hindlimb of rats in the ES group suggests the both trabecular mass and microarchitecture can be well preserved by ES at DRG during unloading period.

In summary, this study has shown that electrical stimulation to the DRG via IMES can mitigate disuse bone loss. Promising results of precise stimulation to DRG with IMES, an effectiveness in reducing disuse bone

loss, and further evidence that CGRP⁺sensory nerves that play an important role in maintaining bone quality were demonstrated. The results suggest potential applications of IMES for the prevention and treatment of musculoskeletal diseases. However, there are limitations to the current study. The animals in this study were treated for only 14 days. Further investigation into the long-term effects, as well as the side effect, of the IMES treatment is needed. The present study shows, but cannot explain why, DRG stimulation can enhance CGRP expression in DRG and reduce bone loss on both the ipsilateral hindlimb concurrently. Further study is required to explore the underlying mechanisms.

Acknowledgments This study was supported by Research Grant Council of Hong Kong (Earmarked Research Grant PolyU N_PolyU537/10) and National Science Foundation of China (51061160501).

Conflicts of interest Yuen-Chi Lau, Xing Qian, Kai-Ting Po, Lu-Ming Li, and Xia Guo declare that they have no conflict of interests that are relevant to the work conducted or reported in this manuscript.

References

- LeBlanc AD, Spector ER, Evans HJ, Sibonga JD (2007) Skeletal responses to space flight and the bed rest analog: a review. *J Muscul Neuron Inter* 7:33–47
- Akhter MP, Alvarez GK, Cullen DM, Recker RR (2011) Disuse-related decline in trabecular bone structure. *Biomech Model Mechanobiol* 10:423–429
- McManus MM, Grill RJ (2011) Longitudinal evaluation of mouse hind limb bone loss after spinal cord injury using novel, in vivo, methodology. *J Vis Exp*.
- Collet P, Uebelhart D, Vico L, Moro L, Hartmann D et al (1997) Effects of 1- and 6-month spaceflight on bone mass and biochemistry in two humans. *Bone* 20:547–551
- Laib A, Barou O, Vico L, Lafage-Proust MH, Alexandre C et al (2000) 3D micro-computed tomography of trabecular and cortical bone architecture with application to a rat model of immobilisation osteoporosis. *Med Biol Eng Comput* 38:326–332
- Lecoq B, Potrel-Burgot C, Granier P, Sabatier JP, Marcelli C (2006) Comparison of bone loss induced in female rats by hindlimb unloading, ovariectomy, or both. *Joint Bone Spine* 73:189–195
- Zaidi M, Fuller K, Bevis PJ, GainesDas RE, Chambers TJ et al (1987) Calcitonin gene-related peptide inhibits osteoclastic bone resorption: a comparative study. *Calcif Tissue Int* 40:149–154
- Zaidi M, Chambers TJ, Bevis PJ, Beacham JL, Gaines Das RE et al (1988) Effects of peptides from the calcitonin genes on bone and bone cells. *Q J Exp Physiol* 73:471–485
- Ballica R, Valentijn K, Khachatryan A, Guerder S, Kapadia S et al (1999) Targeted expression of calcitonin gene-related peptide to osteoblasts increases bone density in mice. *J Bone Miner Res* 14:1067–1074
- Imai S, Matsusue Y (2002) Neuronal regulation of bone metabolism and anabolism: calcitonin gene-related peptide-, substance P-, and tyrosine hydroxylase-containing nerves and the bone. *Microsc Res Tech* 58:61–69
- Brooks JW, Thompson SW, Rice AS, Malcangio M (2004) (S)-AMPA inhibits electrically evoked calcitonin gene-related peptide (CGRP) release from the rat dorsal horn: reversal by cannabinoid receptor antagonist SR141716A. *Neurosci Lett* 372:85–88
- Ren JC, Fan XL, Song XA, Zhao XH, Chen MX et al (2012) Prolonged hindlimb unloading leads to changes in electrophysiological properties of L5 dorsal root ganglion neurons in rats after 14 days. *Muscle Nerve* 45:65–69
- Zerath E, Canon F, Guezennec CY, Holy X, Renault S et al (1995) Electrical stimulation of leg muscles increases tibial trabecular bone formation in unloaded rats. *J Appl Physiol* 79:1889–1894
- Hong-wei H, Lu-ming L, Bo-zhi M, Zhao-yang C, Fang-jun L et al (2008) A programmable and implantable neuro-stimulator. *Space Medic Med Engin* 21:147–151
- Qian X, Hao H, Ma B, Wen X, Hu C et al (2012) Programmable and implantable neurostimulator with novel stimulus waveforms for rat models. *Electron Lett* 48:1036–1038
- Zhang JM, Homma Y, Ackerman WE, Brull SJ (2001) Topical application of acidic bupivacaine to the lumbar ganglion induces mechanical hyperalgesia in the rat. *Anesth Analg* 93:466–471, 464th contents page
- Shields RK, Dudley-Javoroski S, Law LA (2006) Electrically induced muscle contractions influence bone density decline after spinal cord injury. *Spine* 31:548–553, Phila Pa 1976
- Nelson BR, Claes K, Todd V, Chaverra M, Lefcort F (2004) NELL2 promotes motor and sensory neuron differentiation and stimulates mitogenesis in DRG in vivo. *Dev Biol* 270:322–335
- Sugama S, Fujita M, Hashimoto M, Conti B (2007) Stress induced morphological microglial activation in the rodent brain: involvement of interleukin-18. *Neuroscience* 146:1388–1399
- Florijn RJ, Slats J, Tanke HJ, Raap AK (1995) Analysis of antifading reagents for fluorescence microscopy. *Cytometry* 19:177–182
- Bloomfield SA, Allen MR, Hogan HA, Delp MD (2002) Site- and compartment-specific changes in bone with hindlimb unloading in mature adult rats. *Bone* 31:149–157
- Bikson M, Rahman A, Datta A, Fregni F, Merabet L (2012) High-resolution modeling assisted design of customized and individualized transcranial direct current stimulation protocols. *Neuromodulation* 15:306–315